**Original Research**

# MRI of Iron-Oxide Labelled Transplanted Hepatocytes in Mice: Effect of Treatment with Cyclophosphamide

Isabelle Leconte, MD,[1]* Stéphane Pallu, PhD,[1] Jorge Abarca-Quinones, MSc,[1] Nicolas Michoux, PhD,[1] Frank Peeters, PhD,[1] Kim Radermacher, PhD,[2] Christine Sempoux, MD, PhD,[3] Mustapha Najimi, PhD,[4] Etienne Sokal, MD, PhD,[4] and Bernard E. Van Beers, MD, PhD[1]

**Purpose:** To assess if 1.5T MRI can be used to study the transport to the liver, the intrahepatic distribution and engraftment of iron-oxide labelled hepatocytes in cyclophosphamide-treated and untreated mice.

**Materials and Methods:** Hepatocytes were isolated from C57bl/6 mice and were labelled with 1.63 μm iron-oxide particles. Seventeen mice were pretreated with cyclophosphamide to disrupt the sinusoidal endothelium and 15 were left untreated. Seven days after splenic injection of the labelled hepatocytes, T2*-weighted gradient-echo images at 1.5T were acquired. The hepatic transport, distribution and engraftment of the labelled hepatocytes were assessed with signal intensity (SI) and T2* measurements, electron paramagnetic resonance (EPR), texture analysis and histology.

**Results:** Lower hepatic SI ($P = 0.005$), lower T2* ($P = 0.033$) and larger number of particles at histology ($P = 0.006$) suggested increased transport to the liver of labelled hepatocytes in cyclophosphamide-treated mice versus untreated mice. At histology, most particles were located in Kupffer cells. Particles distribution was heterogeneous. No difference between both groups was observed at texture analysis.

**Conclusion:** MRI is useful to assess the transport to the liver and intrahepatic distribution of transplanted labelled hepatocytes. The preferential location of iron-oxide particles within Kupffer cells after seven days limits the value of MRI for assessing hepatocyte engraftment.

**Key Words:** hepatocyte; cyclophosphamide; MR imaging; transplantation; liver
**J. Magn. Reson. Imaging 2010;32:367–375.**


LIVER TRANSPLANTATION is an effective treatment of acute or chronic liver failure and liver-based inherited metabolic diseases. However, the procedure has substantial morbidity and mortality and the demand for transplanted livers is higher than the supply of donated cadaver organs. The supply of adult living donors may somewhat abate the organ shortage, but is not without significant risk to the donor and recipient (1). Transplantation of isolated liver cells has been evaluated as a less invasive alternative to organ transplantation or as a bridge for patients who are waiting for a donor liver (2–9). Liver cell transplantation has many advantages. Several patients can be treated with one donor, less immunosuppressive treatment is required, cell transplantation can be repeated if necessary, and hepatocytes can be cryopreserved and used in emergencies in contrast to intact livers.

The feasibility and safety of liver cell transplantation in humans have been shown in individual case reports (3,4,10–13). Liver biopsy with immunohistochemical analysis is currently used to monitor the transport to the liver, the intrahepatic distribution and outcome of transplanted hepatocytes. A noninvasive alternative to liver biopsy is MRI after transplantation of hepatocytes labelled ex vivo with iron-oxide particles. The feasibility of detecting the susceptibility-induced signal changes resulting from the presence of iron-oxide particles within the transplanted hepatocytes with in vivo MRI has been recently shown in animals (14,15). Iron-oxide particles of different sizes have been used for this purpose. Compared to dextran-coated nanometer-sized iron-oxide particles, polymer-coated micron-sized iron-oxide particles have

[1]Radiodiagnostic Unit, Université Catholique de Louvain, Brussels, Belgium.
[2]Biomedical Magnetic Resonance Unit, Université Catholique de Louvain, Brussels, Belgium.
[3]Department of Pathology, Université Catholique de Louvain, Brussels, Belgium.
[4]Laboratory of Pediatric Hepatology and Cell Therapy, Université Catholique de Louvain, Brussels, Belgium.
Isabelle Leconte and Stéphane Pallu contributed equally to this work.
*Address reprint requests to: I.L., MD, Radiodiagnostic Unit, Université Catholique de Louvain, St-Luc University Hospital, Avenue Hippocrate 10, B-1200 Brussels, Belgium. E-mail: isabelle.leconte@uclouvain.be
Received June 17, 2009; Accepted April 29, 2010.
DOI 10.1002/jmri.22255
Published online in Wiley InterScience (www.interscience.wiley.com).

the advantages of providing higher iron levels within the cells and being inert, allowing long-term studies of labelled cells and their progeny (14). Both intraportal and intrasplenic hepatocyte injections (16,17) lead to efficient hepatocyte transport to the liver (18). Most transplanted hepatocytes (70–85%) are destroyed in the small portal branches and liver sinusoids within 24 to 48 hours (19) and residual cells entrapped in the sinusoids can produce ischemia-reperfusion with activation of Kupffer cells (20,21). The surviving fraction of cells enters the liver plate and eventually engrafts within the liver parenchyma (22). Manipulations aimed at disruption of the endothelial barrier improve hepatocyte engraftment. These manipulations include the use of cyclophosphamide which disrupts the hepatic sinusoidal endothelium of the liver sinusoids without obvious effect on hepatocyte function. Ex vivo studies performed by Malhi et al (23) showed that hepatocyte engraftment was improved in rats treated with cyclophosphamide compared with control rats.

We aimed to assess if 1.5T MRI can be used to quantitatively study the transport to the liver, the intrahepatic distribution and engraftment of 1.63 μm-diameter iron-oxide labelled hepatocytes transplanted in cyclophosphamide-treated and untreated mice.

## MATERIALS AND METHODS

### *Animals*

The study was approved by the ethics committee for animal use of our institute. A total of 40 C57bl/6 mice (Elevage Janvier, Le Genest Saint Isle, France) were used for the study. Seventeen mice treated with cyclophosphamide (Endoxan; Baxter, Lessines, Belgium) and 15 untreated mice were grafted with iron-oxide labelled hepatocytes. Four additional cyclophosphamide-treated mice were sacrificed before hepatocyte transplantation to assess the effect of cyclophophamide on the endothelial barrier. Treated mice received 200 mg/kg cyclophosphamide intraperitonally 48 hours before hepatocyte transplantation or sacrifice. Four SHAM (control) mice were also imaged by MRI and transmission electron microscopy (TEM) without receiving hepatocytes.

### *Cell Isolation and Labelling*

Hepatocytes were isolated by standard collagenase perfusion from two-month old male mice and were repeatedly centrifugated according to the method of Seglen (24). The hepatocytes were suspended and cultured in Williams E medium (Gibco Invitrogen, Paisley, UK) with 10% v/v fetal, heat inactivated bovine serum (Gibco Invitrogen), 2 mM glutamine (Sigma Aldrich, St Louis, MO, USA), 0.875 μM bovine insulin (Sigma Aldrich), 100 nM dexamethasone (Sigma Aldrich), 100 μg/ml streptomycin (Gibco Invitrogen), 100 UI/ml penicillin (Gibco Invitrogen), and 5 ng/ml epidermal growth factor (Sigma Aldrich). Cells were plated in 1 $\mu g/cm^2$ type I collagen-coated culture flasks (Biocoat; Becton Dickinson Labware, Bedford, UK) at a density of 2.5 $10^6$ cells/60 mm-diameter plate and allowed attaching. Medium was changed after four hours. To magnetically label the cells, 1.63 μm-diameter (6 $\mu l/10^6$ cells, at iron concentration of 4.5 $10^9$ pg/mL), carboxylic acid (COOH) functionalized, polystyrene/divinyl benzene-coated iron-oxide particles (Bangs laboratories, Fishers, IN, USA) were added directly to the culture flask three hours after the medium was changed and incubated for 18 hours.

Cells were washed twice with phosphate-buffered saline solution at pH 7.4 (Gibco Invitrogen) to remove loosely bound free particles after labelling. Cells were then released from the dish by incubation with 0.05% w/v trypsin/ethylene diamine tetraacetic acid (EDTA) (Gibco Invitrogen). After centrifugation, cells were resuspended at $10^6$ cells/mL. Cell viability was tested by trypan blue (Sigma Aldrich) exclusion.

To separate free particles from labelled cells, the cells were pelleted, and resuspended in the complete growth Williams E medium at $10^6$ cells/mL, before performing density centrifugation through Ficoll-Paque Plus (Amersham Biosciences, Piscataway, NJ, USA) as described by Shapiro et al (25–27). Briefly, 3 mL of Ficoll-Paque Plus was put into 15 mL plastic Falcon tubes. Then 3 mL of resuspended cells were gently layered on top of the Ficoll-Paque Plus with care taken not to disturb the interface. The tubes were centrifuged at 400*g* and 4°C, for 25 minutes. After centrifugation, most free particles and dead cells had pelleted to the bottom of the tube. Viable cells were localized at the layer between Ficoll-Paque Plus and growth medium. The cells were removed with a plastic pipette, placed in a 15 mL Falcon tube and viability was again assessed with the trypan blue exclusion test. The cells were washed with growth medium to remove trace of Ficoll-Paque Plus. After five minutes centrifugation at 400*g* and 4°C, the cells were resuspended in phosphate-buffered saline solution at pH 7.4 to obtain a concentration of $10^6$ cells/100 μL and placed in ice. The effect of iron-oxide particle loading on cell viability was also assessed by cell counting 24 hours after replating the labelled cells in type I collagen coated culture flasks.

The location of iron-oxide particles in hepatocytes was determined in vitro by optic microscopy. Because of their large size, the iron-oxide particles were detected without staining as brown dots within the cells.

### *TEM*

To assess the effect of cyclophosphamide on the endothelial cells, four mice were sacrificed 48 hours after cyclophosphamide injection and their livers were examined at TEM. Four SHAM mice without cyclophosphamide injection were also sacrified to control the endothelium. Liver fragments of 1 $mm^3$ were fixed for 24 hours in a 2.5% glutaraldehyde solution in 0.1 M sodium cacodylate buffer, pH 7.4. Thereafter, they were washed three times for 30 minutes in the same buffer and postfixed for four hours at 4°C in a 1% w/v osmium tetroxide solution in 0.1 M sodium cacodylate buffer, pH 7.4. Fragments were then embedded in Epon and semi-thin sections were stained with toluidine blue and selected by observation under an Olympus microscope. Ultra-thin sections were contrasted

with 1% w/v uranyl acetate before examination in TEM with a Zeiss EM 109 microscope (Carl Zeiss, Oberkochen, Germany).

### *Hepatocyte Transplantation and MRI*

The recipient mice were operated under general anesthesia, induced by intraperitoneal injection of 0.2 mL of a mixture of 0.9 mL ketamine hydrochloride (Pfizer, Brussels, Belgium), 0.2 mL xylazine hydrochloride (Rompun, Bayer, Leverkusen, Germany), and 3.8 mL saline. A small incision was performed at the site of the spleen. The spleen was partly pushed out. Then, 100 μL of hepatocyte suspension ($10^6$ cells/mouse, + 4°C) was injected into the tip of the spleen with a 27-gauge needle during one minute. The spleen was gently pushed back in the abdomen and the incision was closed.

MRI was performed with a 1.5T Achieva scanner (Philips; Best, the Netherlands) under general anesthesia. Imaging was done one week after cell transplantation. This time period allows for hepatocyte engraftment within the liver (18,28). The mice were placed in a 23-mm diameter microscopic surface coil. The liver was located on single shot gradient-echo images acquired with the following parameters: three orthogonal stacks of five slices with: repetition time/echo time (TR/TE) = 16/8 msec, flip angle = 25°, field of view = 150 mm, slice thickness = 4 mm, 256 × 128 matrix. Three-dimensional T2*-weighted gradient-echo images of the liver were obtained with: TR/TE = 32/14 msec, flip angle = 15°, signal averages = 4 and resolution = 210 × 210 × 400 μm. Multi-echo transverse T2*-weighted gradient-echo images were also acquired with the following parameters: TR/TE = 1525/99 msec, number of echoes = 31, echo spacing = 6.16 msec, flip angle = 30°, signal averages = 4, three slices of 3 mm without gap and in-plane resolution = 200 μm. Respiratory triggering was not used but respiratory artefacts were limited by general anesthesia and signal averaging during MR acquisition. The total acquisition time for the protocol was about 45 minutes.

### *Imaging Data Analysis*

The software *Image J* (a public domain Java image processing program developed by the National Institutes of Health, http://rsbweb.nih.gov/ij/) was used for the segmentation of the regions of interest (ROI's). On each image, one ROI covering the whole liver and one in the paraspinal muscle respectively were drawn manually by a radiologist with 10-year experience in abdominal radiology. The ROI delineating the liver was drawn with care taken to avoid large vessels. The radiologist was blinded to the results of histology and electron paramagnetic resonance (EPR). A signal intensity (SI) ratio, noted $SI_{liver/muscle}$, was calculated as the mean SI measured in the liver divided by the mean SI measured in the muscle. The transverse relaxation time T2* of the liver was determined by fitting a bi-exponential decay to the magnitude of the SI versus echo time plots using homemade software written in Matlab (v. 6.5, rel. 13, MathWorks, Natick, MA, USA). A bi-exponential model was used to account for the presence of blood in the selected ROIs.

The visual aspect of the hepatic tissues with MRI was assessed with Haralick's statistics (29). Eleven (textural) features describing the grey levels interdependence in the image, namely, the energy, the entropy, the contrast, the homogeneity, the correlation, the inverse difference moment, the sum average, the sum variance, the sum entropy, the difference variance, and the difference entropy were estimated (30,31). The Key-Res Technology software (http://www.keyres-technologies.com/index.html) was used for calculating the mean value (over all pixels in the ROI covering the liver) of the 11 textural features. The software parameters included the distance of one pixel between two neighboring pixels, the average of the angular relationships on the four main directions, and the use of five bits of grey levels.

### *Histological Analysis*

After imaging, the mice were sacrificed. Large fragments of the left and caudate lobes were deep-frozen for EPR measurements. The remaining liver and the spleen were fixed in 4% v/v formaldehyde. All liver lobes and spleens were embedded in paraffin, and 5 μm sections were obtained. Hematoxylin-eosin staining was performed using standard techniques and sections were viewed through a microscope (Light Reichert-Jung, Neovarz, Germany).

A semi-quantitative scoring system (from 0: absence of iron-oxide particles to 4: numerous particles) was used to assess the presence of iron-oxide particles on the histological sections. The specific location of iron particles (hepatocytes or Kupffer cells) was determined. Presence of iron-oxide particles at histology was assessed by an experienced pathologist who was blinded to the results of MRI and EPR analysis.

### *EPR*

In EPR, the spectral area is proportional to the total iron mass and the mean iron concentration can be calculated (32). The frequency of the oscillating field used for EPR was 9 GHz. Crushed liver fragments were placed in a 1-mm tube in an EMX EPR spectrometer (Bruker, Rheinstetten, Germany) and the iron concentration was expressed in mmol/mL. The EPR analysis was performed by a chemist who was blinded to the results of MRI and histology.

### *Statistical Analysis*

Numerical variables are expressed as mean ± standard deviation. $SI_{liver/muscle}$ and T2* measurements were compared for the three groups. A Kruskal Wallis test followed by two-by-two comparisons with a Wilcoxon rank-sum test was performed. Bonferroni adjustment was not applied as such adjustment is not recommended in small sample size (33). Wilcoxon rank-sum test was also used to compare histological score and EPR measurements in cyclosphosphamide-

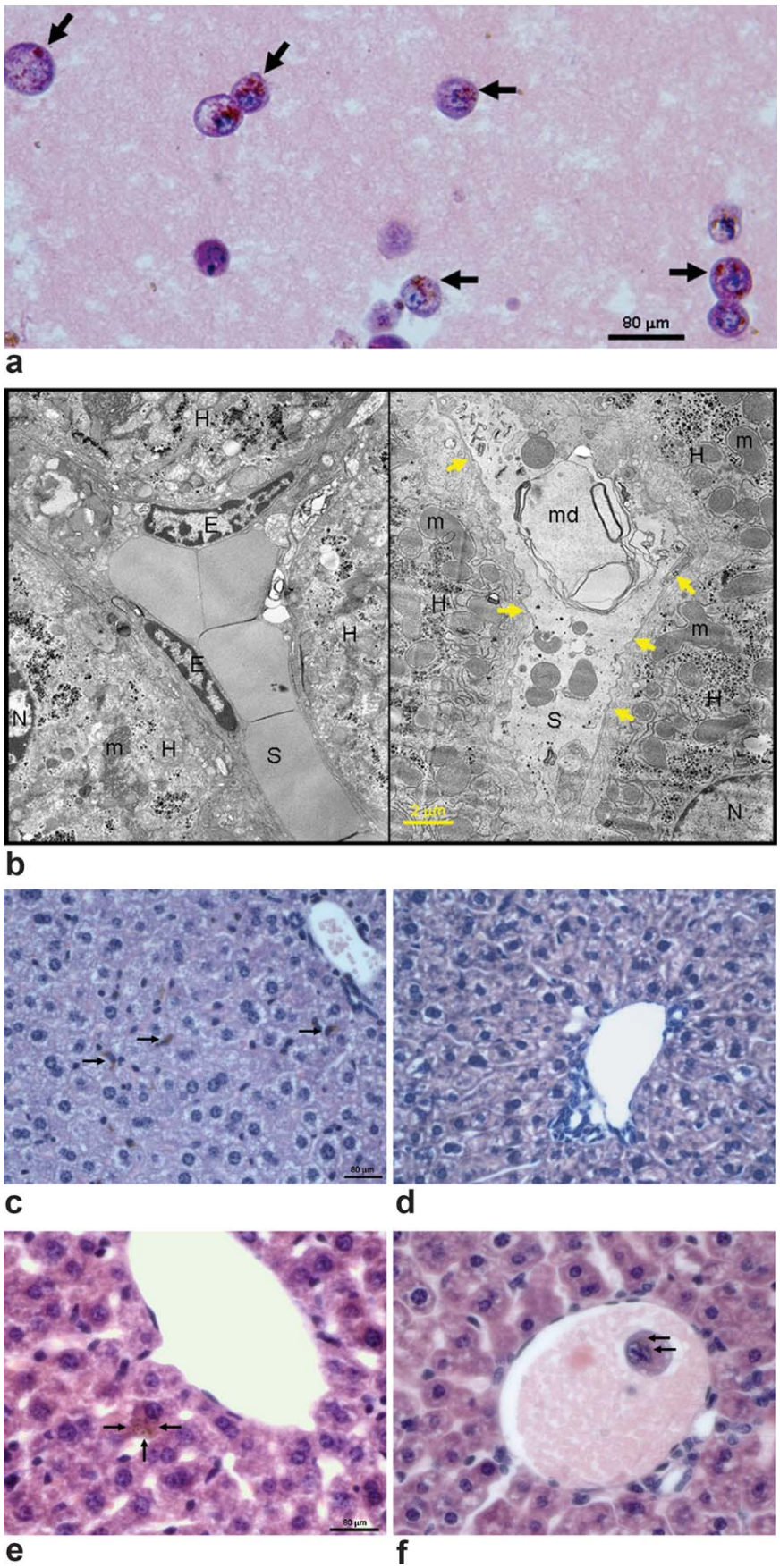


**Figure 1.** Cytological and histological analysis. **a:** Smear of hepatocytes after labelling with iron-oxide particles. The iron-oxide particles clearly appear in brown color in the cytoplasm of the hepatocytes (arrows). **b:** Transmission electron micrograph of a liver sinusoid without (left) and 48 hours after injection of 200 mg/kg cyclophosphamide (right) where the disruption of the sinusoidal endothelium is clearly seen. Structures: hepatocytes (H), endothelial cells (E), sinusoid (S), mitochondria (m), nucleus (N), membrane debris (md). **c:** Light micrograph stained with haematoxylin-eosin in untreated mice transplanted with iron-oxide labelled hepatocytes. The iron oxide particles are detected in Kupffer cells (arrows) (magnification × 40). **d:** Light micrograph stained with haematoxylin-eosin in normal liver (magnification × 40). **e:** Light micrograph stained with haematoxylin-eosin in cyclophosphamide-treated mice shows hepatocyte containing iron-oxide particles integrated into the parenchyma of the liver (arrows) (magnification × 200). **f:** Light micrograph stained with haematoxylin-eosin in cyclophosphamide-treated mice shows hepatocyte containing iron-oxide particles in the portal vein (arrows) (magnification × 200).

Table 1
Mean Values (±SD) of the Parameters Measured at Histology, Electron Paramagnetic Resonance (EPR) and MRI

| | Pretreated grafted mice | Untreated grafted mice | Control ungrafted mice |
|---|---|---|---|
| Histological score | 2.83 ± 0.41 | 1.75 ± 0.97 | – |
| EPR (mmol/mL) | $0.54\ 10^{-5} \pm 0.94\ 10^{-5}$ | $0.43\ 10^{-5} \pm 0.67\ 10^{-5}$ | – |
| T2* (msec) | 12 ± 3.5 | 15 ± 3.9 | 23 ± 0.5 |
| $SI_{liver/muscle}$ | 0.49 ± 0.03 | 0.62 ± 0.05 | 1.00 ± 0.08 |

treated mice versus untreated mice. Finally, spearman coefficients were used to assess the correlations between all parameters for cyclosphosphamide-treated mice and untreated mice. A $P$ value $< 0.05$ was regarded as statistically significant for all tests cited above.

For texture analysis, principal component (PC) analysis was performed (31). The method generates a new set of variables (the PCs) based on a linear combination of the original variables. The first PC accounts for as much of the variability in the data as possible while each succeeding PC accounts for as much of the remaining variability as possible. Mapped into this new system of coordinates (where axes follow the direction of greatest variance in the data set) the mean vectors of the texture features are better represented, and differences between groups, if they exist, can be better visualized. As one can not know a priori how many and which textural features are important to describe the images, features were divided into several sets of different size $N$ (from $N = 11$ to $N = 3$). Therefore, different numbers and combinations of textural features were submitted to PC analysis. All calculations were done with Matlab.

## RESULTS

### *In Vitro Results*

The viability of hepatocytes was 44 ± 2% after trypsine/EDTA treatment and the viability of the remaining hepatocytes was 80 ± 3% after Ficoll-Paque Plus density centrifugation. Iron-oxide particles were present in 84 ± 2 % of the viable hepatocytes after density centrifugation. Cell viability after labelling, replating and 24-hours cell seeding was 79 ± 6%.

Cytological analysis confirmed iron-oxide uptake within the hepatocytes after simple incubation without transfecting agents. The iron-oxide particles were located in the cytoplasm (Fig. 1a). It was observed at electron microscopy that cyclophosphamide disrupted the endothelial barrier of the hepatic sinusoids (Fig. 1b). There was a coexistence of normal and altered endothelial cells in the same mice.

### *MRI*

$SI_{liver/muscle}$ and T2* measurements are shown in Table 1. After injection of hepatocytes labelled with iron-oxide particles, the $SI_{liver/muscle}$ was significantly lower ($P = 0.005$) in the 15 cyclophosphamide-treated mice compared to the 19 untreated mice. The signal intensities of these two groups of transplanted mice were significantly lower than those in the ungrafted mice ($P < 0.003$) (Fig. 2, top).

The T2* relaxation times were significantly lower ($P = 0.033$) in the cyclophosphamide-treated mice relative to the untreated mice. The relaxation times of these two groups were significantly lower than those in the ungrafted mice ($P < 0.007$) (Fig. 2, middle).

SI in the liver was found homogeneous in control ungrafted mice (Fig. 3a). The distribution of iron-oxide particles within the liver was heterogeneous and varied from one mouse to another mouse in both groups of mice grafted with iron-oxide labelled hepatocytes (Fig. 3b and c). Textural features are summarized in Table 2. In grafted mice, the high values associated with the entropy compared to the homogeneity feature and the low values associated with the energy and correlation features, show that within the liver grey level transitions are rather numerous, large and not uniformly distributed. In control mice, conversely, the higher values associated with the energy and homogeneity and the lower values associated with the entropy and contrast demonstrate that the visual aspect of the hepatic tissue is more uniform, less granular, and less contrasted. PC analysis (Fig. 2, bottom) shows a significant overlap in the results of cyclophosphamide-treated and untreated mice groups, whereas the control mice group is well separated from the previous groups. This result suggests that it is not possible to differentiate the texture features of the hepatic tissue between cyclophosphamide-treated and untreated mice. In contrast, the texture of the control mice differs significantly from that of the transplanted mice.

### *Histology*

Most of the iron-oxide particles were localized in Kupffer cells (Fig. 1c which can be compared with Fig. 1d of normal liver). Few hepatocytes containing iron-oxide particles were detected in the livers of cyclophosphamide-treated and untreated mice (Fig. 1e). Few hepatocytes containing iron-oxide particles were also detected in the portal vein of both mice groups (Fig. 1f). Iron-oxide scoring was significantly higher in the cyclophosphamide-treated mice than in the untreated mice ($P = 0.006$, Table 1).

### *EPR Measurements*

Mean iron concentrations in the cyclophosphamide-treated mice and untreated mice did not differ significantly ($P = 0.8$, Table 1).

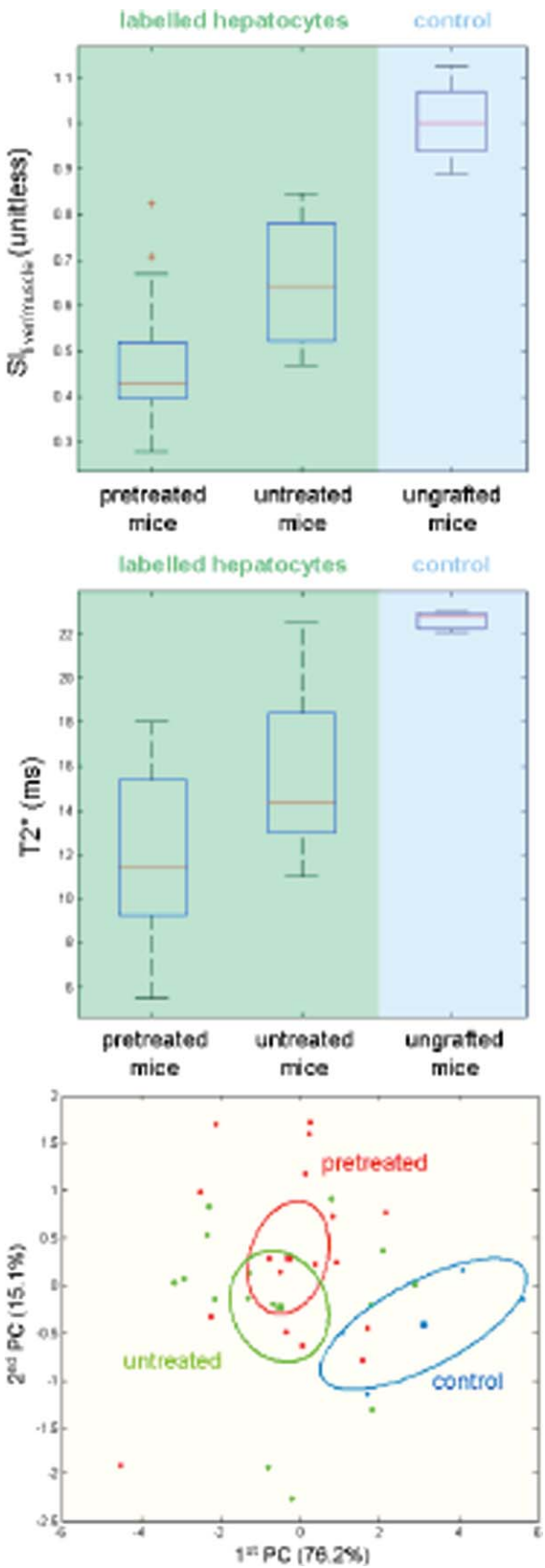


### *MRI and Histological Correlation*

There was a weak negative correlation between the $SI_{liver/muscle}$ and the histological scoring ($P = 0.03$, $r = -0.4$) for both populations of cyclophosphamide-treated and untreated mice. Moderate negative correlations were found between T2* and the EPR measurements ($P = 0.003$, $r = -0.5$) and between T2* and the histological scoring ($P = 0.02$, $r = -0.5$) for both populations.

## DISCUSSION

The first observation in this study was the lower SI and T2* in cyclophosphamide-treated than in untreated mice. This observation can be explained by a higher transport to the liver of iron oxide particles (and thus labelled hepatocytes) in the former group as significant more iron-oxide particles were observed in cyclophosphamide mice than in untreated mice at histopathological analysis. The increased transport of iron-oxide labelled hepatocytes to the liver of mice treated with cyclophosphamide might be explained by lower portal pressure in this group. Indeed, it is known that the deposition of hepatocytes within the liver sinusoids causes transient portal hypertension. This hypertension is resolved by the integration of the transplanted cells within the liver plate (34). Vasodilators and vascular disrupting agents such as cyclophosphamide may decrease the portal hypertension and therefore facilitate further transport of hepatocytes to the liver (35).

Differences in geometrical arrangement of iron-oxide particle clusters (36) between cyclophosphamide-treated and untreated mice might be another explanation for the observed differences in SI and relaxation times between the two groups. However, we did not observe any difference in the geometrical arrangement of the particles at microscopic level. We think that differences in liver concentration of iron-oxide particles rather than differences in geometry explain the lower SI and T2* in the cyclophosphamide group as suggested by the higher amount of iron-oxide particles in this group at histology and the similar distribution

**Figure 2.** Statistical analysis. **Top** and **middle:** $SI_{liver/muscle}$ and T2* measurements are shown respectively. Boundary of boxes closest to zero indicates 25th percentile, line within boxes indicates median, and boundary of boxes farthest from zero indicates 75th percentile. Error bars indicates smallest and largest value within 1.5 box lengths of 25th and 75th percentiles. Outliers are represented as individual crosses. All differences between groups are statistically significant. **Bottom:** The texture features are mapped into a system of coordinates defined by the first two PCs (accounting all together for 91.3% of the total variability in the data). Separation between groups is assessed with 95% tolerance ellipses (ellipses gravity centres are displayed with square markers). It is observed that the variables explaining cyclophosphamide-treated and untreated mice data overlap, while variables explaining control mice data (and grouping them into an eccentric cluster) are significantly different.

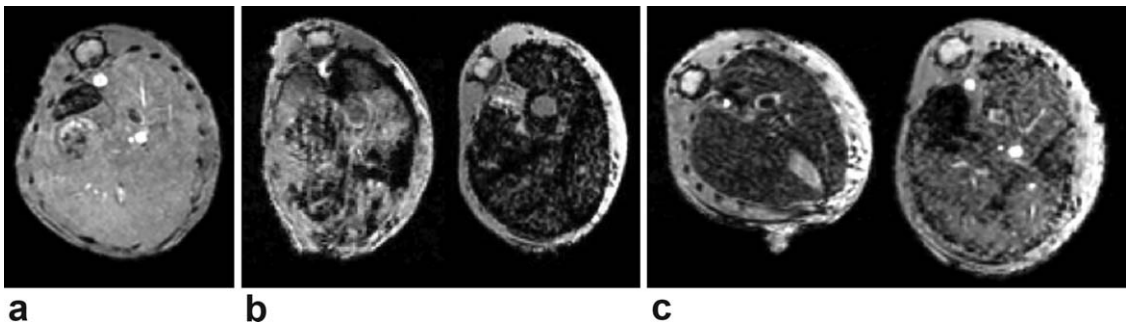


**Figure 3.** Magnetic resonance imaging analysis. **a:** In vivo 3D FFE image (TR/TE = 32/14 msec) of the liver of a control ungrafted mouse. Signal in the liver is homogeneous. **b:** In vivo 3D FFE images (TR/TE = 32/14 msec) of the liver of two mice pretreated with cyclophosphamide and transplanted with iron-oxide labelled hepatocytes. Distribution of iron-oxide particles is heterogeneous in the liver and differs between the two mice. **c:** In vivo 3D FFE images (TR/TE = 32/14 msec) of the liver of two untreated mice transplanted with iron-oxide labelled hepatocytes. Distribution of iron-oxide particles is heterogeneous in the liver and differs between the two mice.

between cyclophophamide-treated and untreated mice at texture analysis.

The second observation is that the vast majority of the iron-oxide particles were located within Kupffer cells and not within hepatocytes. The preferential location of the iron-oxide particles within the Kupffer cells has not been previously reported in the radiological literature. However, this finding is not unexpected. After transplanted hepatocytes are transported to the liver within the first hours after splenic injection, they are entrapped in the periportal sinusoids where a small proportion of the hepatocytes pass the endothelial barrier to engraft by seven days and repopulate the liver. It is known that 70% to 85% of the hepatocytes die in the sinusoids within the first 24 to 48 hours after transplantation and are taken up by the Kupffer cells (15,26,37). Our findings are in accordance with these data. One week after transplantation, we observed that most iron-oxide particles were located within Kupffer cells at histological examination. The distribution of the iron oxide particles as seen at MRI after one week reflects thus the previous history of transport to the liver and sinusoidal entrapment of the grafted hepatocytes. It does, however, not reflect the current location of the surviving hepatocytes, as most iron oxide particles are not within hepatocytes but within Kupffer cells.

This result underscores a fundamental limitation of the use of iron-oxide labelled cells: the inability of differentiating between iron-oxide particles located in living cells and iron-oxide particles in dead cells or in macrophages one week after cell transplantation. Therefore, MRI of iron-oxide labelled cells may be useful to assess the early transport to the liver and intrahepatic distribution of transplanted cells, but not to assess later stages of cell engraftment and liver repopulation. For assessing these later stages, imaging methods using reporter genes that are expressed only in living cells may be more suitable (38). Landis et al (39) showed that liver repopulation by transplanted hepatocytes could be assessed by 31P spectroscopy after transfecting the hepatocytes with the creatine kinase gene.

The third observation in this study was the heterogeneous distribution of iron-oxide particles within the liver, without significant differences between cyclophosphamide-treated and untreated mice at texture analysis. Shapiro et al (26) measured the properties of labelled cells at a higher spatial resolution on 7.0 and 11.7T MR systems. They observed circular shapes of dark contrast in MR images in one mouse after dead labelled hepatocytes injection, and uniformly (or not) dispersed dark clusters in nine mice after living labelled hepatocytes injection. Luciani et al (15) used a different protocol (transplanted mice with labelled hepatocytes with nanosized iron-oxide particles injected in the portal vein) but similar sequence with a 1.5T human MR system. Our MR images with labelled cells (Fig. 3b) and theirs appear similar qualitatively. Images show heterogeneous hypointense clusters scattered throughout the liver parenchyma. This heterogeneous distribution is quantitatively demonstrated in our study by the low values of homogeneity and inverse differential moment, as well as the high values in contrast and entropy relative to these values in control mice.

Table 2
Mean Values (±SD) of the Textural Features*

| | Energy | Entropy | Contrast | Homogeneity | Correlation | Inverse difference moment |
|---|---|---|---|---|---|---|
| Pretreated mice | 9.80 ± 3.81 | 233 ± 7.41 | 19.9 ± 6.71 | 95.0 ± 12.3 | 21.1 ± 10.6 | 94.9 ± 13.5 |
| Untreated mice | 9.59 ± 4.76 | 233 ± 9.48 | 19.1 ± 6.77 | 94.3 ± 14.9 | 32.9 ± 8.54 | 92.6 ± 16.8 |
| Control mice | 21.7 ± 6.51 | 212 ± 11.0 | 14.5 ± 4.80 | 118 ± 13.0 | 30.2 ± 7.76 | 120 ± 14.6 |

*Features values are normalized within 0–255 range. Energy measures the local uniformity of the grey levels. Entropy measures the randomness of the grey levels. Contrast measures the amount of grey levels variations. Homogeneity increases with less contrast. Correlation measures the linear dependency of grey levels of neighbouring pixels. Inverse difference moment measures the local homogeneity of the grey levels.

Our study has several limitations. We did not observe significant differences in iron concentration between cyclophosphamide-treated and untreated mice with EPR. This can be explained by the technique of sampling. Indeed, only samples of two hepatic lobes were analyzed with EPR and the distribution of iron-oxide particles was heterogeneous. We used micron-sized divinyl benzene coated iron-oxide particles because of their higher relaxivity and stability compared to nanosized commercially available iron-oxide particles. As our study suggests that iron-oxide particles are not useful for long-term studies, the use of stable iron-oxide particles may be questioned. Transplanted hepatocytes are known to be fragile. In future studies, it may be better to use stem cells because they are more resistant (40). However, stem cells have never been used in patients with hepatic disease and we wanted to improve the understanding of a method already used in patients. MRI data acquired with a 1.5T human MR system have lower resolution than those acquired with high field animal scanners, but are interesting to assess the potential future applications of this technique in human.

In conclusion, MRI can be used to assess the transport to the liver and intrahepatic distribution of transplanted hepatocytes labelled with iron-oxide particles as shown by differences of SI and T2* measurements between cyclophosphamide-treated and untreated mice, and by differences in visual texture between control mice and mice with iron labelled hepatocytes. However, one week after transplantation, most of those particles were located within Kupffer cells. Therefore, the role of MRI in assessing the engraftment of iron-oxide labelled hepatocytes in the liver may be questioned.

## ACKNOWLEDGMENT

We thank Céline Caillau (Laboratory of Pediatric Hepatology and Cell Therapy, Université Catholique de Louvain, Brussels, Belgium) for her excellent technical assistance in the murine hepatocyte isolation.

## REFERENCES

1. Fox IJ, Roy-Chowdhury J. Hepatocyte transplantation. J Hepatol 2004;40:878–886.
2. Najimi M, Sokal EM. Liver cell transplantation. Minerva Pediatr 2005;57:243–257.
3. Fox IJ, Chowdhury JR, Kaufman SS, et al. Treatment of the Crigler-Najjar syndrome type I with hepatocyte transplantation. N Engl J Med 1998;338:1422–1426.
4. Muraca M, Gerunda G, Neri D, et al. Hepatocyte transplantation as a treatment for glycogen storage disease type 1a. Lancet 2002; 359:317–318.
5. Sokal EM, Smets F, Bourgois A, et al. Hepatocyte transplantation in a 4-year-old girl with peroxisomal biogenesis disease: technique, safety, and metabolic follow-up. Transplantation 2003;76:735–738.
6. Stéphenne X, Najimi M, Sibille C, et al. Sustained engraftment and tissue enzyme activity after liver cell transplantation for argininosuccinate lyase deficiency. Gastroenterology 2006;130:1317–1323.
7. Horslen SP, Fox IJ. Hepatocyte transplantation. Transplantation 2004;77:1481–1486.
8. Fox IJ, Roy-Chowdhury J. Hepatocyte transplantation. Am J Transplant 2004;4:7–13.
9. Lee SW, Wang X, Chowdhury NR, et al. Hepatocyte transplantation: state of the art and strategies for overcoming existing hurdles. Ann Hepatol 2004;3:48–53.
10. Grossman M, Raper SE, Wilson JM. Transplantation of genetically modified autologous hepatocytes into nonhuman primates: feasibility and short-term toxicity. Hum Gene Ther 1992;3: 501–510.
11. Holzman MD, Rozga J, Neuzil DF, et al. Selective intraportal hepatocyte transplantation in analbuminemic and Gunn rats. Transplantation 1993;55:1213–1219.
12. Rozga J, Holzman MD, Moscioni AD, et al. Repeated intraportal hepatocyte transplantation in analbuminemic rats. Cell Transplant 1995;4:237–243.
13. Horslen SP, McCowan TC, Goertzen TC, et al. Isolated hepatocyte transplantation in an enfant with a severe urea cycle disorder. Pediatrics 2003;111:1262–1267.
14. Shapiro EM, Skrtic S, Koretsky AP. Sizing it up: cellular MRI using micron-sized iron oxide particles. Magn Reson Med 2005; 53:329–338.
15. Luciani A, Parouchev A, Smirnov P, et al. In vivo imaging of transplanted hepatocytes with a 1.5-T clinical MRI system – initial experience in mice. Eur Radiol 2008;18:59–69.
16. Wang J, Li W, Min J, et al. Intrasplenic transplantation of allogeneic hepatocytes modified by BCL-2 gene protects rats from acute liver failure. Transplant Proc 2004;36:2924–2926.
17. Sigot V, Mediavilla MG, Furno G, et al. A simple and effective method to improve intrasplenic rat hepatocyte transplantation. Cell Transplant 2004;13:775–781.
18. Ponder KP, Gupta S, Leland F, et al. Mouse hepatocytes migrate to liver parenchyma and function indefinitely after intrasplenic transplantation. Proc Natl Acad Sci USA 1991;88:1217–1221.
19. Joseph B, Malhi H, Bhargava KK, et al. Kupffer cells participate in early clearance of syngeneic hepatocytes transplanted in the rat liver. Gastroenterology 2002;123:1677–1685.
20. Lemasters JJ, Thurman RG. Reperfusion injury after liver preservation for transplantation. Annu Rev Pharmacol Toxicol 1997;37: 327–338.
21. Serracino-Inglott F, Habib NA, Mathie RT. Hepatic ischemia-reperfusion injury. Am J Surg 2001;181:160–166.
22. Gupta S, Rajvanshi P, Sokhi R, et al. Transport to the liver and integration of transplanted hepatocytes in rat liver plates occur by disruption of hepatic sinusoidal endothelium. Hepatology 1999;29:509–519.
23. Mahli H, Annamaneni P, Slehria S, et al. Cyclophosphamide disrupts hepatic sinusoidal endothelium and improves transplanted cell engraftment in rat liver. Hepatology 2002;36:112–121.
24. Seglen PO. Hepatocyte suspensions and cultures as tools in experimental carcinogenesis. J Toxicol Environ Health 1979;5: 551–560.
25. Shapiro EM, Skrtic S, Sharer K, et al. MRI detection of single particles for cellular imaging. Proc Natl Acad Sci USA 2004;101: 10901–10906.
26. Shapiro EM, Sharer K, Skrtic S, et al. In vivo detection of single cells by MRI. Magn Reson Med 2006;55:242–249.
27. Shapiro EM, Skrtic S, Koretsky AP. Long term cellular MR imaging using micron sized iron oxide particles. In: Proceedings of the 12th Annual Meeting of ISMRM, Kyoto, Japan, 2004 (Abstract 1734).
28. Yamanouchi K, Zhou H, Roy-Chowdhury N, et al. Hepatic irradiation augments engraftment of donor cells following hepatocyte transplantation. Hepatology 2009;49:258–267.
29. Haralick RM, Shanmugam K, Dinstein I. Textural features for image classification. IEEE Trans Sys Man Cybern 1993;SMC-3: 610–621.
30. Zizzari A, Seiffert U, Michaelis B, et al. Detection of tumor in digital images of the brain. In: Proceedings of the IASTED International Conference on Signal Processing, Pattern Recognition and Applications SPPRA, Rhodes, Greece, 2001;132–137.
31. Jirák D, Dezortová M, Taimr P, et al. Texture analysis of human liver. J Magn Reson Imaging 2002;15:68–74.
32. Radermacher KA, Beghein N, Boutry S, et al. In vivo detection of inflammation using pegylated iron oxide particles targeted at E-selectin. A multimodal approach using MR imaging and EPR spectroscopy. Invest Radiol 2009;44:398–404.
33. Nakagawa S. A farewell to Bonferroni: the problem of low statistical power and publication bias. Behav Ecol 2004;15:1044–1045.

34. Rajvanshi P, Kerr A, Bhargava KK, et al. Efficacy and safety of repeated hepatocyte transplantation for significant liver repopulation in rodents. Gastroenterology 1996;111:1092–1102.
35. Slehria S, Rajvanshi P, Ito Y, et al. Hepatic sinusoidal vasodilators improve transplanted cell engraftment and ameliorate microcirculatory perturbations in the liver. Hepatology 2002;35: 1320–1328.
36. Rad AM, Arbab AS, Iskander ASM, Jiang Q, Soltanian-Zadeh H. Quantification of superparamagnetic iron oxide (SPIO)-labeled cells using MRI. J Magn Reson Imaging 2007;26:366–374.
37. Allen KJ, Soriano HE. Liver cell transplantation: the road to clinical application. J Lab Clin Med 2001;138:298–312.
38. Serganova I, Ponomarev V, Blasberg R. Human reporter genes: potential use in clinical studies. Nucl Med Biol 2007;34:791–807.
39. Landis CS, Yamanouchi K, Zhou H, et al. Noninvasive evaluation of liver repopulation by transplanted hepatocytes using 31P MRS imaging in mice. Hepatology 2006;44:1250–1258.
40. Ju S, Teng GJ, Lu H, et al. In vivo MR tracking of mesenchymal stem cells in rat liver after intrasplenic transplantation. Radiology 2007;245:206–215.